Physical, morphological, and biological studies on PLA/nHA composite nanofibrous webs containing Equisetum arvense herbal extract for bone tissue engineering

By: Khakestani, M (Khakestani, Maliheh)[1,2] ; Jafari, SH (Jafari, Seyed Hassan)[1] ; Zahedi, P (Zahedi, Payam)[1] ; Bagheri, R (Bagheri, Reza)[3] ; Hajiaghaee, R (Hajiaghaee, Reza)[4]

View ResearcherID and ORCID

JOURNAL OF APPLIED POLYMER SCIENCE
Volume: 134 **Issue:** 39
Article Number: 45343
DOI: 10.1002/app.45343
Published: OCT 15 201
View Journal Impact

JOURNAL OF APPLIED POLYMER SCIENCE

Impact Factor

1.86 *2016* **1.727** *5 year*

JCR® Category	Rank in Category	Quartile in Category
POLYMER SCIENCE	36 of 86	Q2

Data from the 2016 edition of Journal Citation Reports

Publisher
WILEY, 111 RIVER ST, HOBOKEN 07030-5774, NJ USA

ISSN: 0021-8995
eISSN: 1097-4628

Research Domain
Polymer Science

Close Window

Abstract

A series of herbal extract
successfully prepared by
nanohydroxyapatite (nHA
nanofibrous webs under
average diameter of 157
of the webs was carried
scanning electron micros
scanning calorimetry (DS
prepared webs were also
(pH 7.2) medium. Moreo
adipose tissue-derived m
and proliferation of AT-M
Osteogenic differentiatio
phosphatase activity and
PLA nanofibrous webs, t
modulus were increased
adhesion was observed
PLA/nHA/EE webs show
3 times higher than that of PLA/nHA and tissue culture polystyrene as control, respectively. (c) 2017 Wiley Periodicals, Inc. J. Appl. Polym. Sci. 2017, 134, 45343.

Keywords

Author Keywords: biocompatibility; biodegradable; biomedical applications; biopolymers and renewable polymers; structure-property relationships

KeyWords Plus: DRUG-DELIVERY; PROLIFERATION; DIFFERENTIATION; ANTIBACTERIAL; REGENERATION; FLAVONOIDS; SCAFFOLDS

Author Information

Reprint Address: Jafari, SH (reprint author)

+ Univ Tehran, Sch Chem Engn, Dept Polymer, Coll Engn, POB 11155-4563, Tehran, Iran.

Addresses:

+ [1] Univ Tehran, Sch Chem Engn, Dept Polymer, Coll Engn, POB 11155-4563, Tehran, Iran

Citation Network

0 Times Cited

32 Cited References

View Related Records

Create Citation Alert

(data from Web of Science Core Collection)

Times Cited Counts

All Databases
Web of Science Core Collection
BIOSIS Citation Index
Chinese Science Citation abase
Data Citation Index
Russian Science Citation Index
SciELO Citation Index

ge Count

180 Days: 57
e 2013: 57
n more

record is from:
of Science Core Collection
ence Citation Index Expanded

uggest a correction

If you would like to improve the quality of the data in this record, please suggest a correction.

[2] Payame Noor Univ, Dept Chem, POB 19395-4697, Tehran, Iran

[3] Sharif Univ Technol, Dept Mat Sci & Engn, Tehran, Iran

[4] ACECR, Inst Med Plants, Med Plants Res Ctr, Karaj, Iran

E-mail Addresses: shjafari@ut.ac.ir

Funding

Funding Agency	Grant Number
Iran Nanotechnology initiative Council	

View funding text

Publisher

WILEY, 111 RIVER ST, HOBOKEN 07030-5774, NJ USA

Categories / Classification

Research Areas: Polymer Science

Web of Science Categories: Polymer Science

Document Information

Document Type: Article

Language: English

Accession Number: WOS:000405633000010

ISSN: 0021-8995

eISSN: 1097-4628

Journal Information

Impact Factor: Journal Citation Reports

Other Information

IDS Number: FA7NI

Cited References in Web of Science Core Collection: 32

Times Cited in Web of Science Core Collection: 0

Journal of Applied Polymer Science

Physical, morphological, and biological studies on PLA/nHA composite nanofibrous webs containing *Equisetum arvense* herbal extract for bone tissue engineering

Maliheh Khakestani,[1,2] Seyed Hassan Jafari,[1] Payam Zahedi,[1] Reza Bagheri,[3] Reza Hajiaghaee[4]

[1]Department of Polymer, School of Chemical Engineering, College of Engineering, University of Tehran, P.O. Box 11155-4563, Tehran, Iran

[2]Department of Chemistry, Payame Noor University, P.O. Box 19395-4697, Tehran, Iran

[3]Department of Materials Science and Engineering, Sharif University of Technology, Tehran, Iran

[4]Medicinal Plants Research Center, Institute of Medicinal Plants, ACECR, Karaj, Iran

Correspondence to: S. H. Jafari (E-mail: shjafari@ut.ac.ir)

ABSTRACT: A series of herbal extract incorporated into poly(lactic acid) (PLA) composite nanofibrous scaffolds were successfully prepared by using electrospinning technique. *Equisetum arvense* extract (EE) and nanohydroxyapatite (nHA) in different quantities were loaded into PLA solution to fabricate composite nanofibrous webs under various electrospinning conditions. Uniform nanofibers were obtained with an average diameter of 157 ± 47 nm in the case of those containing the herbal extract. Characterization of the webs was carried out by means of Fourier transform infrared (FTIR) spectroscopy, field emission-scanning electron microscopy (FE-SEM), energy-dispersive X-ray spectroscopy (EDX), and differential scanning calorimetry (DSC) techniques. Mechanical properties, porosity, and contact angle of the prepared webs were also determined. Releasing behavior was investigated in phosphate buffer solution (pH 7.2) medium. Moreover, cell studies and osteogenic capacity were assessed *in vitro* using human adipose tissue-derived mesenchymal stem cell (AT-MSC). Evaluations of cell attachment, spreading, and proliferation of AT-MSC were done by SEM observation and thiazolyl blue (MTT) assay. Osteogenic differentiation capability of AT-MSC on the nanofibrous webs was analyzed by alkaline phosphatase activity and calcium content assay. It was found that with the addition of nHA and EE to PLA nanofibrous webs, their surface hydrophobicity was reduced while the tensile strength and Young's modulus were increased satisfactorily. Regarding the samples containing EE and nHA, cellular adhesion was observed with flattened normal morphology. Osteogenic differentiation of AT-MSC on PLA/nHA/EE webs showed the highest mineralization capacity after 3 weeks which, was about 1.8 and 3 times higher than that of PLA/nHA and tissue culture polystyrene as control, respectively. © 2017 Wiley Periodicals, Inc. J. Appl. Polym. Sci. **2017**, *134*, 45343.

KEYWORDS: biocompatibility; biodegradable; biomedical applications; biopolymers and renewable polymers; structure-property relationships

Received 14 March 2017; accepted 29 May 2017

DOI: 10.1002/app.45343

INTRODUCTION

Currently, development and improvement of scaffolds in tissue engineering are considered as an essential research area in regenerative medicine. High porosity scaffolds have a substantial role in cell seeding, cell proliferation, spatial formation, and regeneration of new tissues. An ideal scaffold not only should have suitable physical and mechanical properties but also it must be biocompatible and biodegradable. Furthermore, such a scaffold should improve intercellular interactions to assist tissue regeneration.[1]

Electrospinning is a simple and flexible method to produce fibers with average diameters from tens of nanometers to several microns. In recent years, this method has been extensively utilized to produce nanofibers in tissue engineering and drug delivery systems.[2,3] Nanofibers have special properties such as high specific surface area and appropriate porosity, which make them promising candidate for scaffolds. These properties facilitate cell adhesion and growth as well as the transfer of vital substances for cell proliferation. Furthermore, electrospun nanofibers owing to their unique properties simplify diffusion of biomolecules loaded into them to the surroundings and increase the mass transfer. These features have boosted utilization of nanofibers in drug delivery applications.[4]

Biodegradable polyesters such as poly(lactic-*co*-glycolic acid), poly (ε-caprolactone) (PCL), poly(lactic acid) (PLA), and poly(glycolic acid), are considered as most common synthetic

polyesters used in bone tissue engineering and drug delivery.[5–7] Among them, PLA has been widely utilized in bone regeneration applications because of its semicrystalline nature, good strength, low toxicity, and predictable biodegradation rate. The mentioned polymers alone do not provide a proper surface for cell adhesion and growth due to lack of cellular recognizable signals. This deficiency can be eliminated by using bioactive ceramics such as nanohydroxyapatite (nHA) and preparing composite scaffolds.[8] nHA is a phosphate-based ceramic that has a chemical structure similar to the minerals in bone. Using nHA in PLA enhances activity and viability of seeded cells and neutralizes the acidic products of PLA degradation by forming a buffer.[9] It has suitable mechanical properties, osteoconductivity, and biocompatibility. Therefore, it has been extensively used in scaffolds of bone tissue engineering.[9,10] Moreover, nHA improves surface topography, increases cell adhesion and growth, and causes calcium-bearing minerals to participate in boosting the formation of new bone tissue. nHA facilitates the differentiation of mesenchymal stromal cells and osteoblast precursor cell line to osteoblast and increases activities of alkaline phosphatase and osteocalcin expression.[11,12]

In order to benefit from therapeutic properties of medicinal plants and botanicals such as their antioxidant characteristics, anti-inflammatory, and antibacterial attributes, etc., the extracts of these herbs are loaded into the drug delivery systems to make use of their positive effects *in vitro* and *in vivo* via controlled delivery methods.[13–15] Another research area for medicinal herbs is their application in bone regeneration. To improve attachment, proliferation, and differentiation of bone cells, various biomolecules and growth factors have been employed in bone tissue engineering. These will improve bone regeneration at the bone/material interface. Generally, these materials are expensive, degrade easily, and have considerable limitations in widespread applications.[16] Therefore, using active ingredients of medicinal plants in bone regeneration studies have a promising potential as alternative options. There are many pieces of evidence in *in vitro* and *in vivo* studies that show some herb species have a positive effect on bone metabolism.[17–22] As a typical example Suganya *et al.*[17] incorporated petroleum ether extract of *Cissus quadrangularis* (CQ) and nHA in polymeric nanofibers for bone tissue regeneration application. They exhibited that CQ and CQ-nHA loaded PCL nanofibrous scaffolds increased the potential for proliferation and differentiation of human fetal osteoblast cells compared with neat PCL nanofibrous scaffolds and also synergic effect of CQ and nHA was studied. Zhang *et al.*[22] investigated the effect of total flavonoids of *Epimedium koreanum* Nakai on proliferation and differentiation of primary osteoblasts. They reported inhibition of cell proliferation at most concentrations; however, differentiation promotion of primary osteoblasts was observed by accelerating the alkaline phosphatase (ALP) activity. The potential role of some medicinal herbs on proliferation and differentiation of stem cells was also studied.[23] However, the studies on the effect of herbal extract loading on polymeric composite scaffolds for bone tissue engineering applications and evaluation of cell responses are very rare.

Equisetum arvense (EE) plant, also known as horsetail, is a medicinal herb which has antioxidant characteristics, anti-inflammatory, and antibacterial attributes. The herb is considered to have therapeutic effects such as a diuretic, regenerating bone and cartilage as well as preventing osteoporosis.[24] Phytochemical compounds in this plant consist of alkaloids, phytosterols, tannins, triterpenoids, and phenolic compounds. Some flavonoids such as kaempferol, quercetin, apigenin, luteolin, phenolic acids, and styrylpyrones are among phenolic compounds of this plant.[25] This herb has minerals like silica, potassium, manganese, magnesium, and sulfide. Since it has considerable silica content (5%–8%), this plant has great ability to absorb and use protein and facilitates collagen formation. The effect of EE hydromethanolic extracts in bone tissue regeneration was studied by Pereira *et al.*, and showed the dose-dependent effect of the extract on cell viability and ALP activity of human bone marrow cells.[19] In another work, Asgharikhatooni *et al.* reported the effectiveness of topical application of EE ointment in wound healing and reduction of inflammation and pain relieving after episiotomy.[26]

Despite unique specifications of the EE herb and particularly its high osteogenic differentiation potential, so far its application influence as a scaffold for bone tissue engineering has not been explored. Therefore, this work is aimed to explore, for the first time, the beneficial roles of EE herbal plant and influential role of nHA in improving PLA characteristics for making it a suitable candidate as a scaffold for bone tissue engineering. For this purpose hydroethanolic extract of EE was loaded into electrospun PLA and PLA/nHA composite nanofibers and their morphological, physical, and mechanical characteristics were probed via various techniques. Moreover, EE release behavior in phosphate buffer solution (PBS) was investigated. Cell viability and cellular adhesiveness were also determined by culturing of a mesenchymal stem cell isolated from human adipose tissue (AT-MSC). Moreover, osteogenic differentiation capability of AT-MSC on composite nanofibrous scaffolds was assessed by ALP activity and calcium content assays.

EXPERIMENTAL

Materials

PLA grade 2002 D was obtained from NatureWorks in pellet form. This grade of PLA contains both D-lactide and L-lactide isomers. Spherical nHA (KF-HAP04) with average size of 20 to 40 nm and 99% purity was provided by Kinfon Pharma, China. EE plant extract was gathered from north of Iran. Chloroform (CF), dimethylformamide (DMF), and dimethyl sulfoxide (DMSO) were supplied by Merck Co., Germany. All the materials were used without further purification.

Preparation and Characterization of Plant Extract

The hydroethanolic extract was prepared by maceration method. In this procedure, 200 g of the plant was washed, milled, and then transferred into a glass balloon. 1000 mL of extracting liquid, distilled water: ethanol (1:1), was added to the balloon and it remained for 3 days as the maceration process. The final extracted solution was percolated and dried by using a rotary evaporator, operating at 50 °C under reduced pressure. The obtained extract was kept in sterile Petri dish and stored in a refrigerator at 4 °C. The concentration of total flavonoids in the EE was determined using spectrophotometric method.[27] The

total flavonoids content of the extract was expressed in terms of rutin equivalent (mg of RU/g of extract). The amount of silica was measured by atomic absorption method.

Preparation of the Electrospinning Solutions

To prepare PLA pure solution, a weighed amount of PLA granules was dissolved in CF at ambient temperature for 3 h, then DMF and DMSO (3:1) were added to the PLA/CF solution to give a solution concentration of 7.5% (w/v). In order to provide PLA solution containing EE, first EE was dissolved in DMSO and then added to the PLA/CF/DMF solution to obtain an EE-contained solution with a concentration of 10% (w/w). Composite nanofibrous webs containing EE was prepared by loading an appropriate amount of nHA into the solution. For this purpose, different amounts of nHA were dispersed in DMF by sonication for 30 min (Bandelin power 70 W) to prepare polymeric solutions containing 2.5, 5, 7.5, and 10% (w/w) of nHA. Then each dispersed solution was added to EE/DMSO solution, stirred for 5 min, and instantly added to PLA solution dropwise to achieve a series of PLA/nHA/EE mixtures with predetermined concentrations.

Electrospinning Process

For this purpose, the polymeric solution was inserted into a 5 mL of plastic syringe and a high voltage of 15 kV was applied. Electrospinning set up was supplied by Nanoazma Co., Iran, the flow rate was 0.6 mL/h, and the electrospun nanofibers were collected on a rotating aluminum collector kept 20 cm away from the tip of the needle (23 gauge; 0.43 mm inner diameter). The processing parameters were obtained by optimization of preliminary experimental results. The electrospun nanofibers were dried under vacuum for 48 h to evaporate any residual solvents.

Nanofibrous Webs Characterization

FTIR Studies. Attenuated total reflectance Fourier transform infrared (ATR-FTIR) spectroscopic analysis of electrospun nanofibrous webs was performed using a Bruker instrument (Equinox 55LS 101 series, Germany) with the resolution of 4 cm^{-1} (averaging 50 scans) for determination of functional groups of as-prepared nanofibrous webs.

FE-SEM Studies. The electrospun nanofibers were sputter-coated with a thin layer of gold and visualized using a field emission scanning electron microscope (FE-SEM; MIRA3TESCAN-XMU, Czech Republic) with a 20,000× magnification. The average diameter of the electrospun nanofibers was calculated by measuring 30 to 40 individual single nanofibers within each FE-SEM micrographs using image analysis software (ImageJ). Cellular adhesion morphology was also investigated by SEM (VEGA-TESCAN-XMU, Czech Republic) with different magnifications.

Contact Angle Measurements. Hydrophilic/hydrophobic nature of the electrospun nanofibrous webs was determined by water contact angle measurements using a G10 goniometer (Kruss, Germany) at 25 °C and relative humidity of 30%. Average of three measurements was reported.

Porosity Measurements. Density (ρ) was estimated as mass to volume ratio on 20 mm diameter discs cut out of the webs. Three samples were considered for each test. The thickness of samples was measured by Schopper type thickness gauge OSK (model B-12). Porosity (ε) was estimated according to eq. (1), where ρ_0 is the density of neat PLA (1.24 g cm^{-3}). It is to be noted that the density of webs loaded with EE and nHA was found to be close to this value.

$$\varepsilon = \left(1 - \frac{\rho}{\rho_0}\right) \times 100, \quad (1)$$

Thermal Analysis. Thermal behavior was carried out using a differential scanning calorimeter (DSC) (Q100, TA instrument). About 6 to 8 mg of samples were heated from 0 to 200 °C by a heating rate of 10 °C min^{-1} under N_2 atmosphere. Glass transition temperature (T_g), cold recrystallization (T_{cc}), and melting temperatures (T_m) as well as cold crystallization (ΔH_{cc}) and melting (ΔH_m) enthalpies were determined from the second heating scan. The degree of crystallinity (X_c) of the as-produced nanofibrous webs was calculated according to:

$$X_C(\%) = \frac{\Delta Hm - \Delta Hcc}{\Delta H_0} \times 100, \quad (2)$$

where ΔH_{cc} and ΔH_m were derived from the DSC thermograms, ΔH_0 is the theoretical enthalpy of the fully crystalline polymer, for PLA the considered value is 93 J g^{-1}.[28]

Mechanical Properties. The tensile properties of the electrospun nanofibrous webs were determined at ambient temperature using an Instron (model 5566, Amersham, England) with a load cell capacity of 50 N under a crosshead speed of 5 mm/min. The thickness of samples was measured by a Schopper type thickness gauge OSK (model B-12). The webs were cut into rectangular specimens having dimensions of 6 × 30 mm. Three specimens were considered for each electrospun webs. The Young's modulus (E) was evaluated between 0% and 5% of strain. Tensile strength and elongation at break were calculated based on the generated stress–strain curves of each specimen.

***In Vitro* EE Release.** The EE-loaded PLA nanofibrous webs were immersed into 15 mL of PBS at pH = 7.2 under gentle shaking at 37 °C. About 20 mg of EE-loaded PLA/nHA nanofibrous webs were immersed into 15 mL of PBS. At prespecified time intervals, 3 mL of supernatant was taken and immediately replaced with 3 mL of the fresh PBS in order to keep the volume constant. The obtained supernatants were analyzed by a UV–vis spectrophotometry at a wavelength of 275 nm. The cumulative release percentage curve was plotted versus time. The cumulative amount of EE released from the samples was assessed using the following equation:

$$\text{Cumulative EE released } (\%) = \frac{\sum_{t=0}^{t} M_t}{M_{\text{total}}} \times 100, \quad (3)$$

where M_t is the amount of EE released from the webs at time t, and M_{total} is the total amount of EE loaded into the electrospun PLA webs. The entrapment efficiency of EE in PLA nanofibrous webs was about 0.68. This entrapment efficiency has been considered for calculating the reported release data.

Cell Culture and Differentiation. AT-MSCs were cultured in Dulbecco's modified Eagle medium supplemented with 2 m*M* of L-glutamine, 1% of penicillin-streptomycin, and 10% of fetal

bovine serum. The pH of the medium was adjusted to 7.2 to 7.4 by $NaHCO_3$ (all reagents were supplied by Gibco). Composite nanofibrous webs with and without EE were cut into circular scaffolds with a diameter of 1.5 cm and sterilized under UV irradiation for 40 min on each side and soaked in cell culture medium overnight prior to cell seeding to improve protein adsorption and cell attachment. The cells seeded on the scaffolds at a cell density of 2×10^4 cells/well and incubated at 37 °C in 5% of CO_2 for cell proliferation. For osteogenic differentiation evaluation, cell-scaffold constructs were cultured in standard culture medium (Dulbecco's modified Eagle medium supplemented with 10% of fetal bovine serum) which was supplemented with 0.2 m*M* of ascorbic acid 2-phosphate, 100 n*M* of dexamethasone, and 10 m*M* of β-glycerophosphate (all reagents were supplied by Sigma-Aldrich, Pilsburg, The Netherlands). Tissue culture polystyrene (TCP) was used as a control.

In order to evaluate cell attachment on the composite nanofibrous scaffolds with and without EE, chemical fixation of cells was performed for each sample. After 7 days of incubation, the scaffolds were rinsed twice with PBS and afterward fixed in 2.5% of glutaraldehyde for 1 h. Thereafter each sample was rinsed with distilled water and dehydrated with ethanol for 10 min. Finally, the samples were held in a vacuum chamber and then sputter coated with a thin layer of gold for cell morphology observation by using SEM.

MTT Assay. The viability of cultured AT-MSCs was carried out using the colorimetric 3-(4,5-dimethyl-2-thyazol-2-yl)-2,5-diphenyl tetrazolium bromide (MTT) assay. Regarding MTT assay, the scaffolds put on the bottom of the 24-well plate. Cells (2×10^4 cells/well) were seeded and cultured on the nanofibrous scaffolds and TCP as a control for 1, 4, and 7 days. A total of 50 μL of MTT solution was added to each well and incubated for 4 h. Then 200 μL of DMSO was added to each well to terminate the reaction and dissolve purple crystals (formazan). Then 100 μL of each plate was transferred to 96-well plate and the number of living cells was measured by using an ELISA reader (Dana 3200, Iran) at 570 nm.

ALP Activity. ALP activity was measured by *p*-nitrophenol assay (Pars Azmun Kit, Iran) on days 7, 14, and 21. First, 200 μL of RIPA buffer was added to cell scaffolds and TCP construct to extract total protein of cells, followed by centrifuging (14000 rpm) at 4 °C for 15 min to deposit cell debris. Then 1 mL of *p*-nitrophenyl phosphate solution was added to each sample. The absorbance was read at a wavelength of 405 nm and the activity of the enzyme was expressed as IU/L. ALP provided in the kit is used as a standard.

Calcium Content Assay. The amount of calcium minerals deposited on scaffolds and TCP by AT-MSCs under osteogenic differentiation media was evaluated using calcium content assay. In this method, *o*-cresol phthalein complexone was used as a reagent. 250 μL of HCl (0.6 N) was added to each well to extract calcium and homogenized by shaking, then 20 μL of the solution was taken and 1 mL of the reagent added to it. Calcium content was determined using the solution absorption values at a wavelength of 570 nm and a standard curve prepared by serial dilution of the calcium concentrations.

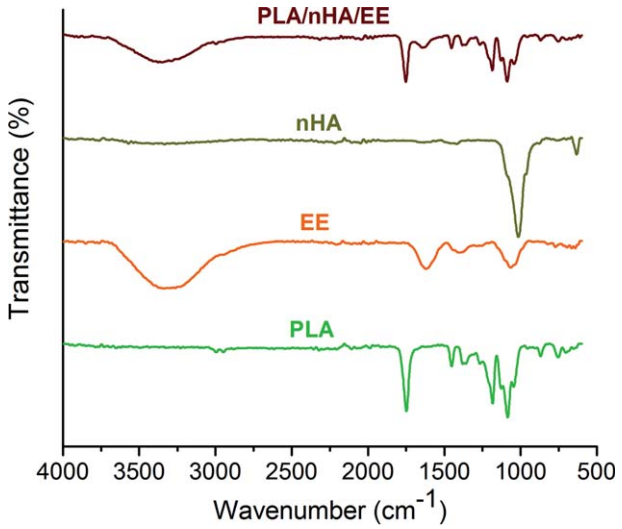

Figure 1. Attenuated total reflectance Fourier transform infrared (ATR-FTIR) spectra of poly(lactic acid) (PLA), *Equisetum arvense* extract (EE), nano hydroxyapatite (nHA), and PLA/nHA/EE nanofibrous webs. [Color figure can be viewed at wileyonlinelibrary.com]

Statistical Analysis

All data were expressed as the mean ± standard deviation. Statistical comparisons were performed by the *t*-test using SPSS software. *P* values <0.05 were considered statistically significant ($n = 3$).

RESULTS AND DISCUSSION

Characterization of EE

The yield of solid residue after extraction and evaporation from 100 g dried plant was determined. The concentration of flavonoids in the EE extracts was investigated using the spectrophotometric method with aluminum chloride. The silica content of the EE was evaluated by atomic absorption. The results show the yield of extraction was 17.5 g per 100 g of dried plant. The total flavonoids and silica contents were 17.51 ± 0.84 mg rutin/g of EE and 564.4 μg/g of EE, respectively.

FTIR Studies of the EE, nHA, PLA Nanofibers, and PLA/nHA/EE Composite Nanofibrous Webs

In order to evaluate the chemical compositions of EE, nHA, PLA nanofibers, and PLA/nHA/EE composite nanofibrous webs their corresponding FTIR spectra are presented in Figure 1. The results reveal the existence of various chemical constituents. The wavenumber (cm^{-1}) of prominent peaks obtained from absorption spectra are described in Table I.

The characteristic peaks of EE are described as follows: the absorption bands in 664 and 771 cm^{-1} were assigned to C—H bonds in alkenes and benzene ring, respectively. The characteristic peak at 1064 cm^{-1} vibration related to C—O bond existing in alcohols, ethers, carbocyclic acids, and esters. C—H bending and stretching vibrations were seen in 1405 and 2925 cm^{-1}. Vibration at 1621 cm^{-1} might be related to C=C in alkenes or conjugated. A broad peak in 3332 cm^{-1} represented hydroxyl group in alcohols, phenols containing hydrogen bonding.

Table I. Characteristic Absorption Bands of EE, PLA, nHA, and PLA/nHA/EE

Characteristic group	EE (cm^{-1})	PLA (cm^{-1})	nHA (cm^{-1})	PLA/nHA/EE (cm^{-1})
C—H (alkenes and benzene ring)	664	703	—	701
	771	754		753
C—C	—	868	—	868
PO_4	—	—	968	—
			1014	
			1070	
C—O (phenol, alcohol, ethers, carboxylic acids, esters)	1064	1045	—	1043
		1084		1087
		1126		1128
		1183		1185
C—H bending vibration	1405	1379	—	1380
		1451		1452
C=C (alkenes, conjugated)	1621	—	—	1644
C=O	—	1748	—	1752
C—H stretching vibration (alkanes)	2925	2947	—	2990
		2994		
O—H (absorbed water, H-bonded)	3332	3334	633	3351
			3334	

In FTIR spectra of PLA, absorption bands for C—H bond were observed at 703 and 754 cm^{-1}. Also, C—O vibration bands were observed at 1045, 1084, 1126, and 1183 cm^{-1}. The C—H bending vibration peaks were observed at 1379 and 1451 cm^{-1}. The maximum absorption peak of C=O characteristic group was seen at 1748 cm^{-1}, C—H asymmetric and symmetric stretching vibration of alkanes were observed at 2947 and 2994 cm^{-1}. Two characteristic peaks of nHA were related to —PO_4 and —OH groups in 1014 and 633 cm^{-1}. Regarding EE incorporated into PLA/nHA composite nanofibrous webs, characteristic chemical bonds of PLA were seen with some changes. The new characteristic peak at 1644 cm^{-1} was detected, this might be due to the

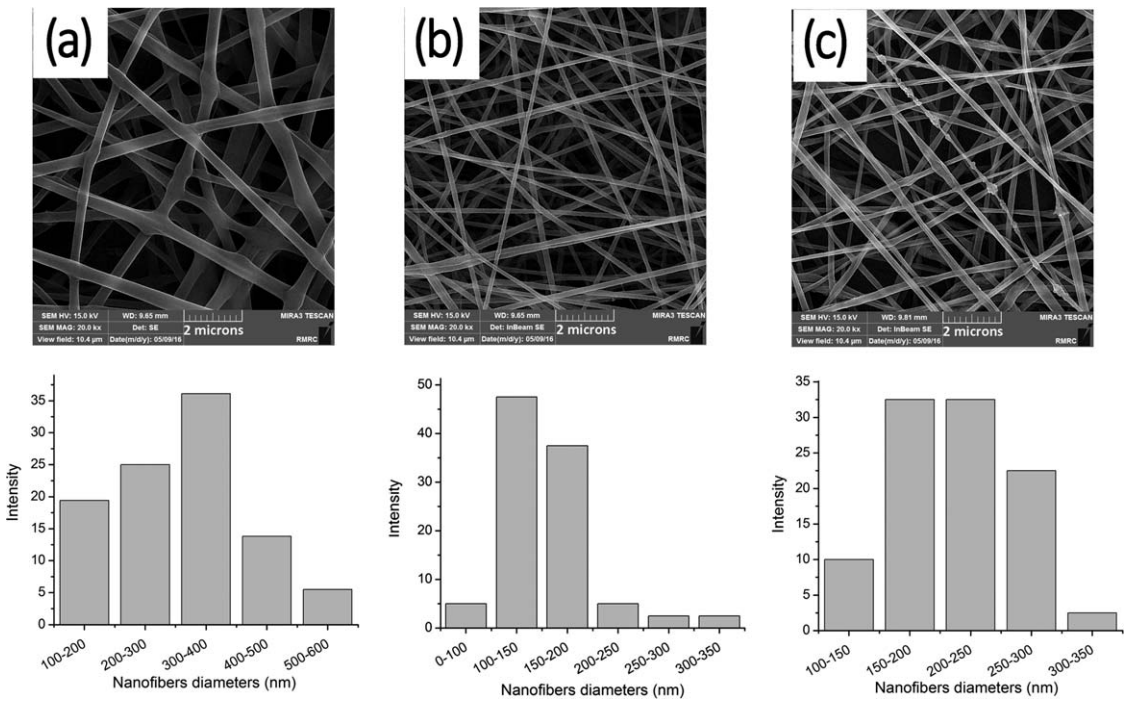

Figure 2. FE-SEM images (a) poly(lactic acid) (PLA), (b) PLA/*Equisetum arvense* extract (EE), and (c) PLA/EE/nanohydroxyapatite (nHA) nanofibers along with their diameter size distribution.

Table II. Physical Properties of PLA, PLA/EE, and PLA/nHA/EE Nanofibrous Webs

Sample	Nanofibers diameter (nm)	Porosity (%)
PLA	316 ± 51	77.5 ± 2.3
PLA/EE	157 ± 47	80.0 ± 3.2
PLA/EE/nHA	217 ± 44	83.4 ± 3.3

C═C interaction of the EE with PLA. Furthermore, the C═O vibration peak of PLA at 1748 cm^{-1} were shifted to 1752 cm^{-1} in the composite nanofibers. These changes could be attributed to the formation of hydrogen bonding between C═O functional group of PLA and OH group of nHA.

Morphological Studies

The morphology of PLA, PLA/EE, and PLA/nHA/EE nanofibers was observed via FE-SEM and the results are represented in Figure 2(a–c). As it is seen, the resulting morphology of the nanofibers containing EE and nHA were appeared beadless, smooth, and homogenous. Size measurements of nanofibers showed that these values were decreased due to the addition of EE to PLA solution. This effect could be attributed to the high conductivity of the solution containing EE. Similar results have been observed by other reseachers.[17] According to the determination of electrical conductivity of PLA and PLA/EE solution, by the addition of EE to PLA solution, the electrical conductivity increased strongly from 1.53 to 29.5 μS cm^{-1}. Herbal extracts mainly contain ionic compounds and therefore their dissolution in a solvent leads to enhancement of electrical conductivity of the solution. The average diameters of nanofibers including PLA, PLA/EE, and PLA/EE/nHA are reported in Table II. By EE incorporation into polymeric solution, the nanofibers diameter was declined. Loading nHA particles into nanofibers led to a slight change in composite nanofibers diameter. Elemental mapping of calcium (Ca) and phosphorus (P) in PLA/nHA composite nanofibers and corresponding EDX spectrum as well as related elemental analysis shown in Figure 3 confirmed presence of nHA and its uniform dispersion within the composite nanofibers.

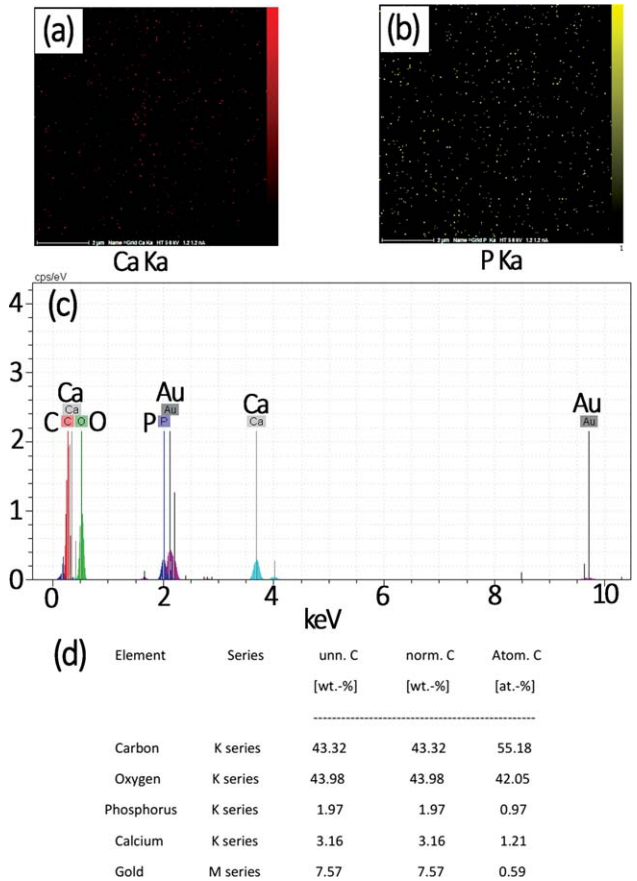

(d)

Element	Series	unn. C [wt.-%]	norm. C [wt.-%]	Atom. C [at.-%]
Carbon	K series	43.32	43.32	55.18
Oxygen	K series	43.98	43.98	42.05
Phosphorus	K series	1.97	1.97	0.97
Calcium	K series	3.16	3.16	1.21
Gold	M series	7.57	7.57	0.59

Figure 3. Elemental mapping of (a) calcium and (b) phosphorus, (c) EDX spectrum and (d) elemental analysis of nanohydroxyapatite (nHA) in poly(lactic acid) (PLA)/nHA composite nanofibers. [Color figure can be viewed at wileyonlinelibrary.com]

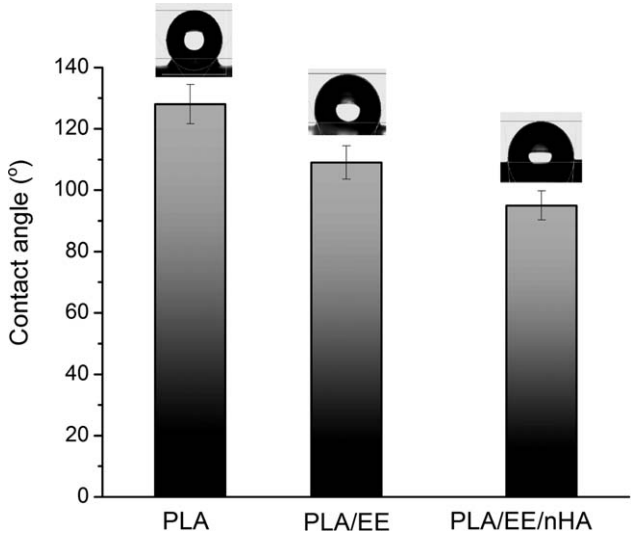

Figure 4. Contact angles of poly(lactic acid) (PLA), PLA/*Equisetum arvense* extract (EE), and PLA/EE/nanohydroxyapatite (nHA) nanofibrous webs.

Scaffolds with high porosity are essential for cell growth and viability. The average porosity values of PLA, PLA/EE, and PLA/EE/nHA nanofibers are shown in Table II. As it can be seen, the porosity of PLA nanofibers was 77.5% and by incorporating EE and nHA, it increased to 80% and 83.4%, respectively. Generally, the reduction in nanofibers diameter could tend to porosity promotion, but in this case, with adding nHA particles porosity increased despite an increase in fibers diameters.

Although composite nanofibers were prepared with different percentages of nHA, just the results related to the optimum percentage i.e., 2.5% are reported here.

Water Contact Angle Measurements of the Nanofibrous Samples

Hydrophilicity has a major effect on cell adhesion. Figure 4 represents contact angle results of nanofibers such as PLA, PLA/EE, and PLA/EE/nHA. The contact angle of PLA nanofibers due to its hydrophobic nature was about 130° which decreased to 95° by incorporation of EE and nHA. These results revealed that EE and nHA due to possessing polar and hydrophilic groups, like

Table III. Thermal Characteristics of PLA, PLA/EE, and PLA/EE/nHA Nanofibrous Webs

Sample	T_g (°C)	T_{cc} (°C)	T_m (°C)	ΔH_{cc} (J/g)	ΔH_m (J/g)	X_C (%)
PLA	62.0	93.9	149.0	16.5	24.7	8.8
PLA/EE	58.2	86.6	151.7	10.3	25.5	16.3
PLA/EE/nHA	58.7	85.1	152.3	11.4	27.5	17.3

carbonyl and hydroxyl, promoted hydrophilicity, and hence, decreased contact angle of PLA.

Thermal Analysis

The thermal characteristics of PLA, PLA/EE, and PLA/EE/nHA nanofibrous webs were obtained by the use of DSC and corresponding data namely T_g, T_{cc}, T_m, ΔH_{cc}, ΔH_m, and X_C are summarized in Table III.

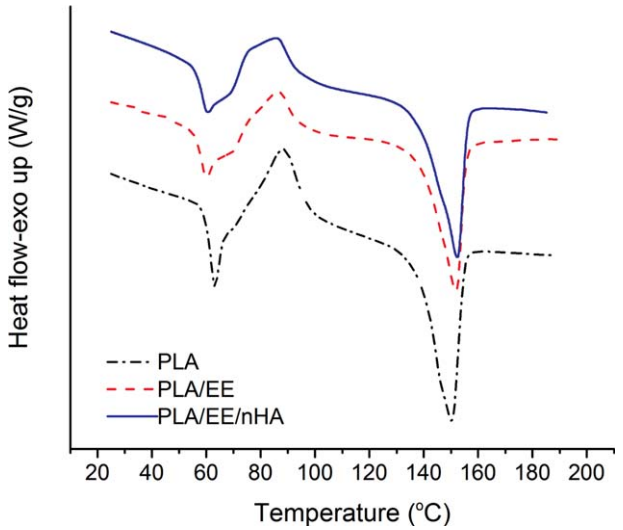

Figure 5. Differential scanning calorimetry (DSC) thermograms of poly(-lactic acid) (PLA), PLA/*Equisetum arvense* extract (EE), and PLA/EE/nanohydroxyapatite (nHA) nanofibers. [Color figure can be viewed at wileyonlinelibrary.com]

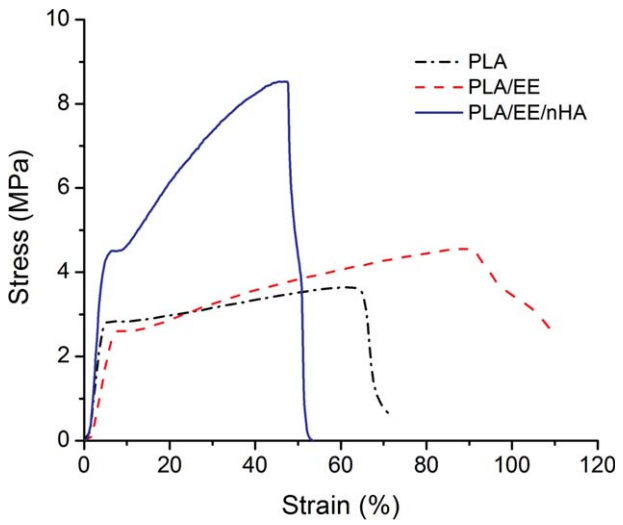

Figure 6. Stress–strain curves of poly(lactic acid) (PLA), PLA/*Equisetum arvense* extract (EE), and PLA/EE/nanohydroxyapatite (nHA) nanofibers. [Color figure can be viewed at wileyonlinelibrary.com]

Also, the DSC thermograms of various nanofibers webs are shown in Figure 5. The appearance of cold recrystallization exothermic peak was due to very low crystallization rate of PLA. As seen, the T_g of PLA/EE nanofibers (58.2 °C) has been decreased. This effect could be related to the plasticizing effect of EE. The T_{cc}s of PLA, PLA/EE, and PLA/EE/nHA were 93.9, 86.6, and 85.1 °C, respectively. The addition of EE and nHA to PLA decreased the cold crystallization enthalpy and shifted T_c to lower temperatures. This observation could be attributed to the slow rate of freezing webs containing EE and nucleating effect of nHA. All samples showed negligible changes in melting temperature as compared to the neat PLA. However, the highest crystallinity belonged to PLA/EE/nHA nanofibers (17.3%). Loading EE into PLA increased its crystallinity from 8.8% to 16.3%. These findings corroborated the nucleation effect of nHA in PLA/EE nanofibers.

Mechanical Properties

The tensile stress–strain curves of PLA, PLA/EE, and PLA/EE/nHA nanofibers are plotted in Figure 6. Tensile strength at yield, Young's modulus, and strain at break are summarized in Table IV. In composite nanofibers, the tensile strength at yield and modulus were increased from 2.7 ± 0.1 MPa and 0.6 ± 0.1 MPa to 4.5 ± 0.4 MPa and 1.7 ± 0.1 MPa, respectively and the strain at break was reduced from 85.6 ± 2.8% to 42.4 ± 4.5% by adding nHA to PLA/EE nanofibers. This could be attributed to inherent high modulus and rigidity of nHA. Incorporation of EE into PLA, as a result of its plasticizing effect, reduced the tensile strength and modulus of PLA and increased its strain at break despite increasing PLA crystallinity. These results were in agreement with similar works.[17]

In Vitro EE Release

Figure 7 displays cumulative release profile of EE from PLA nanofibrous web. As can be seen, at the initial stages a plenty of EE was released. This burst release could be related to low compatibility of hydroethanolic herbal extract with the hydrophobic

Table IV. Tensile Strength, Modulus, and Strain at Break of PLA, PLA/EE, and PLA/EE/nHA Nanofibers

Sample	Tensile strength at yield (MPa)	Young's modulus (MPa)	Strain at break (%)
PLA	2.8 ± 0.0	0.9 ± 0.1	65.7 ± 2.9
PLA/EE	2.7 ± 0.1	0.6 ± 0.1	85.6 ± 2.8
PLA/EE/nHA	4.5 ± 0.4	1.7 ± 0.1	42.4 ± 4.5

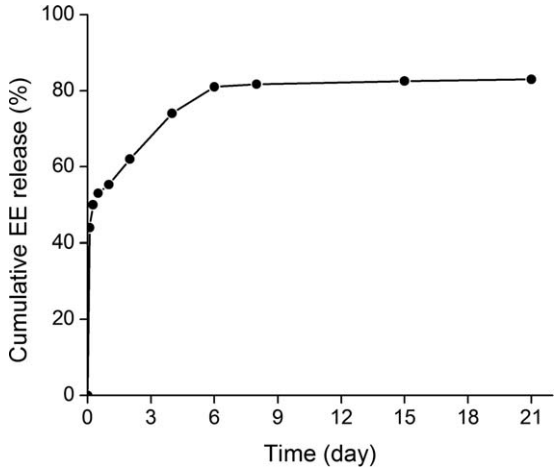

Figure 7. Cumulative release profile of *Equisetum arvense* extract (EE) from poly(lactic acid) (PLA) composite nanofibrous web.

polymer and its adsorption onto the surface of nanofibers. This led to EE accumulation onto the surface, and thus, to the fast release rate in the release media in the early stages of the experiment. The release profile of EE could be categorized into three stages: about 50% of EE was quickly released in the first 3 h (stage 1), and then showed a release with a slower rate (stage 2) followed by approximately a constant release rate (stage 3). However, about 83% of the EE-loaded nanofibers were released within 3 weeks. The remaining of EE will be released by hydrolytic degradation. The results were similar to the findings reported on PLA and their copolymers by other researchers.[29,30]

Morphology and Proliferation of AT-MSC

In order to confirm cell proliferation and adhesion on scaffold surface, SEM observation was conducted. SEM images of AT-MSCs on PLA/nHA and PLA/EE/nHA scaffolds after day 7 of culture are shown in Figure 8(a–f). Due to the desirable effect of nHA on cell adhesion, proliferation and mineralization, biological studies were done on PLA composite nanofibers with and without EE. Cell growth (matured cells) could be observed in two composite nanofibrous scaffolds. The higher magnification images (b, c, e, and f) showed good cell extensions and adhesion on scaffolds. Nanofibers due to the large surface area to the volume have a high potential for cell proliferation. As it is evident, both scaffolds provided suitable conditions for cell growth but the population of AT-MSCs cells proliferated and migrated onto the surface of the PLA/EE/nHA nanofibrous scaffold was qualitatively higher than those of the PLA/nHA scaffolds.

MTT Assay

To assess cell viability, measurements of cell growth were performed. Cell viability onto the surfaces of composite nanofibrous scaffolds with and without EE at days 1, 4, and 7 are displayed in Figure 9. The cells on PLA/EE/nHA composite nanofibrous scaffold compared to TCP and PLA/nHA scaffold have the highest viability. These results and the cell growth images demonstrated the capability of PLA/EE/nHA composite

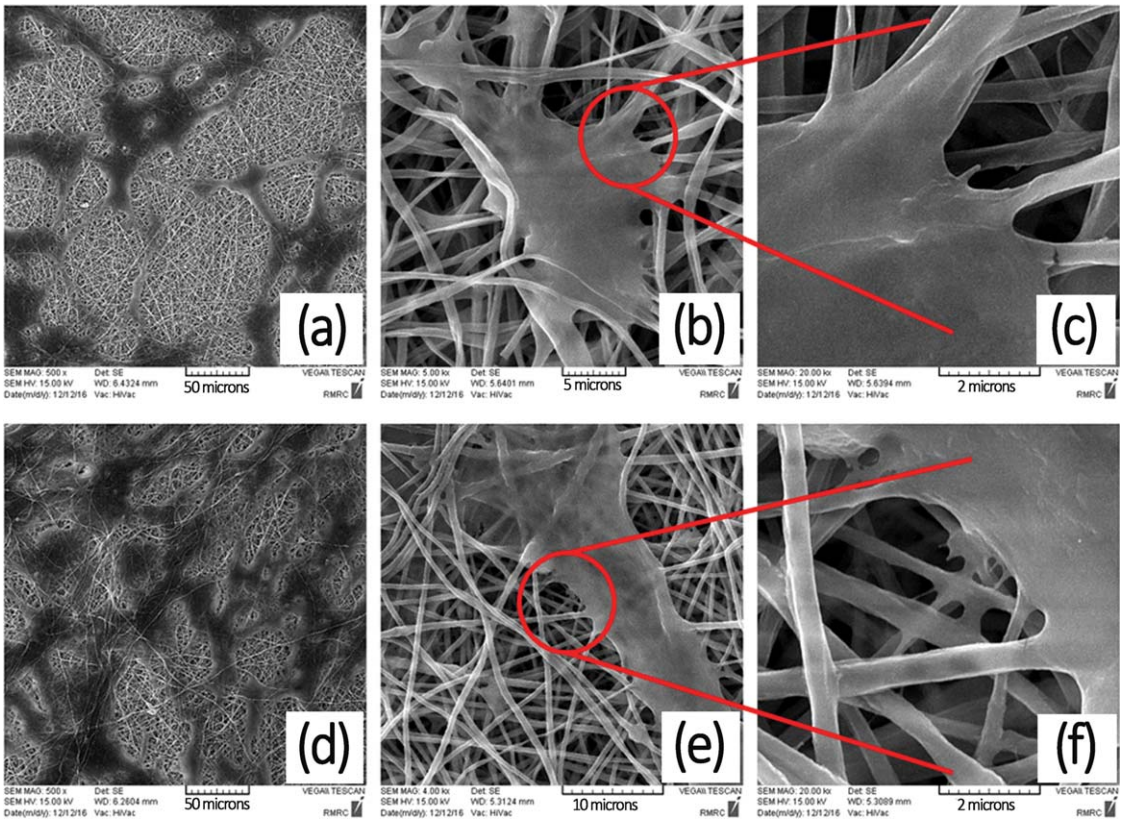

Figure 8. Scanning electron microscopy (SEM) images of human adipose tissue-derived MSC on poly(lactic acid) (PLA)/nanohydroxyapatite (nHA) (a–c) and PLA/*Equisetum arvense* extract (EE)/nHA composite nanofibers (d–f) at day 7. [Color figure can be viewed at wileyonlinelibrary.com]

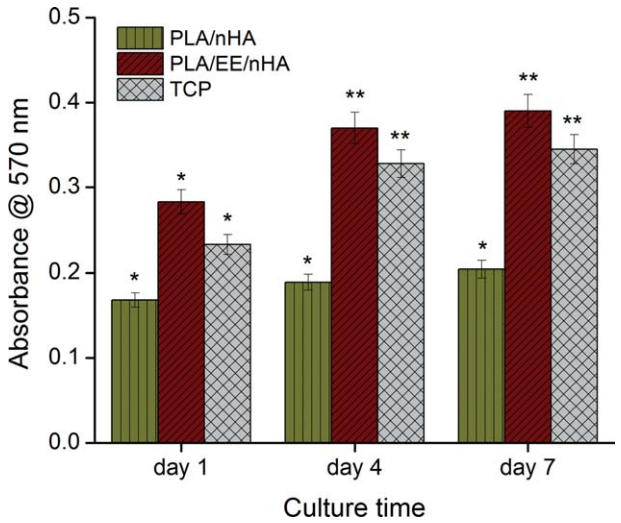

Figure 9. Viability of adipose tissue-derived mesenchymal stem cells (AT-MSCs) onto the surface of poly(lactic acid) (PLA)/nanohydroxyapatite (nHA) composite nanofibrous scaffold with and without *Equisetum arvense* extract (EE) on days 1, 4, and 7 (one and two stars stand for *P* value <0.05 and *P* value >0.1, respectively). [Color figure can be viewed at wileyonlinelibrary.com]

nanofibrous scaffold usage in the biomedical application as scaffolds and drug delivery carriers.

Osteogenic Differentiation

In order to study osteogenic differentiation of AT-MSCs on composite nanofibers and influence of EE on the cell differentiation, two important key markers (ALP activity and calcium content assay) were investigated. Figure 10(a) exhibits ALP activity of AT-MSCs on PLA/nHA, PLA/EE/nHA composite nanofibrous scaffolds, and TCP on days 7, 14, and 21. As can be seen, there was no significant difference between ALP activity of AT-MSCs on both scaffolds and TCP on day 7, but on days 14 and 21, it was higher for scaffolds as compared to TCP. AT-MSCs on composite nanofibrous scaffold containing herbal extract showed the highest amount of ALP activity in those days. Due to the fact that the EE plant contains different components including flavonoids such as kaempferol, quercetin, apigenin, luteolin, etc., and minerals like silica, it seems these compounds improve osteogenic differentiation capacity of AT-MSCs. Similar observations have been reported on ALP activity improvement. Zhang *et al.* reported the positive effect of flavonoids of *Epimedium koreanum* Nakai plant on the differentiation of primary osteoblasts by promoting ALP activity.[22] The effect of quercetin, one of the flavonoids, on increasing osteogenic differentiation in human adipose stromal cells was investigated by Jeong *et al.*[31] Figure 10(b) shows mineralization of AT-MSCs on PLA/nHA and PLA/EE/nHA composite nanofibrous scaffolds. As expected with rising cell culture time in osteogenic media, mineralization of AT-MSCs increased especially on scaffolds containing the extract. Moreover, both PLA/nHA and PLA/EE/nHA composite nanofibers promoted osteogenic differentiation of AT-MSCs, a greater extent of mineral deposition was found in the PLA/EE/nHA composite nanofibers. Osteogenic differentiation of AT-MSC on PLA/EE/nHA scaffolds showed the highest mineralization capacity after 3 weeks, being about 1.8 and 3 times higher than that of PLA/nHA and TCP as control, respectively. Obtained results of differentiation potential increase of AT-MSCs on composite nanofibrous scaffolds containing and free of EE were almost comparable to the results of human fetal osteoblast, hFOB, cell differentiation on PCL/CQ/nHA nanofibrous scaffolds.[17] In the mentioned study when nHA was incorporated into the scaffold containing extract, an acceptable enhance in osteogenic potential was observed. However, in our study the obtained notable improvement in the osteogenic differentiation was due to active components of EE such as flavonoids, which could promote the cell differentiation. It is necessary to note that the considerable increase in mineralization of AT-MSCs on PLA composite nanofibrous scaffolds was obtained while the osteogenic potential of AT-MSCs in comparison with other mesenchymal stem cells

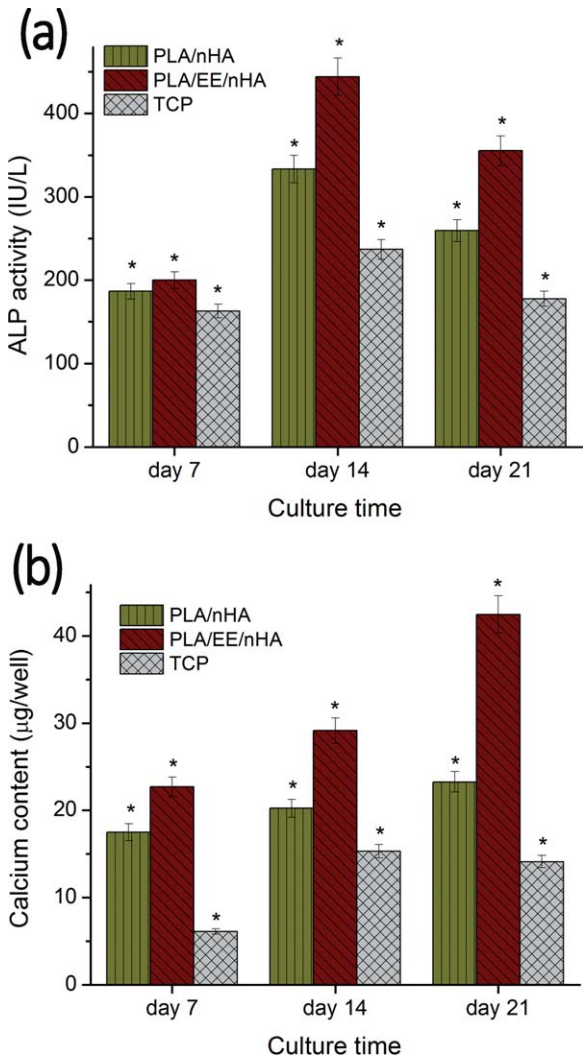

Figure 10. (a) Alkaline phosphatase activity, and (b) quantitative analysis for the mineralization of adipose tissue-derived mesenchymal stem cells (AT-MSCs) on tissue culture polystyrene (TCP), poly(lactic acid) (PLA)/nanohydroxyapatite (nHA), and composite nanofibrous scaffolds on days 7, 14, and 21 (one star stands for *P* value <0.05). [Color figure can be viewed at wileyonlinelibrary.com]

sources such as human fetal mesenchymal stem cells and human umbilical cord mesenchymal stem cells was minimum.[32]

In summary, cellular proliferation and mineralization were indicative of cell ossification and might be due to compounds present in the extract that affected the osteogenic-related signaling pathways.

CONCLUSIONS

In this study, new PLA composite nanofibrous scaffolds containing herbal extract were developed and characterized. FTIR studies showed EE and nHA were successfully loaded into PLA webs. Morphology of the samples was investigated by FE-SEM in which a good dispersion of nHA in composite nanofibers and a significant decrease in fiber diameters were observed. Thermal analysis indicated the plasticizing effect of EE and nucleation effect of nHA in nanofibers. The softening effect of EE in mechanical assessment led to a reduction in modulus and a promotion in strain at break values. However, in composite nanofibrous webs, the addition of nHA increased tensile strength and modulus and at the same time decreased strain at break values. *In vitro* EE release of nanofibers in PBS showed a burst release followed by slower release rate. Composite nanofibrous scaffold containing herbal extract showed excellent cell attachment and promoted proliferation and osteogenic differentiation of AT-MSCs by increasing cell viability, ALP activity, and mineralization content. Our findings indicated that EE extract has a great potential for osteogenic differentiation of AT-MSCs and can be recommended as a suitable candidate for bone tissue engineering application.

ACKNOWLEDGMENTS

The authors thank the Iran Nanotechnology initiative Council for partial support of this work.

REFERENCES

1. Place, E. S.; George, J. H.; Williams, C. K.; Stevens, M. M. *Chem. Soc. Rev.* **2009**, *38*, 1139.
2. Hu, X.; Liu, S.; Zhou, G.; Huang, Y.; Xie, Z.; Jing, X. *J. Controlled Release* **2014**, *185*, 12.
3. Braghirolli, D. I.; Steffens, D.; Pranke, P. *Drug Discov. Today* **2014**, *19*, 743.
4. Sill, T. J.; von Recum, H. A. *Biomaterials* **2008**, *29*, 1989.
5. Puppi, D.; Chiellini, F.; Piras, A. M.; Chiellini, E. *Prog. Polym. Sci.* **2010**, *35*, 403.
6. Hassan, M. I.; Sun, T.; Sultana, N. *J. Nanomater.* **2014**, *2014*, 209049.
7. Aboutalebi Anaraki, N.; Roshanfekr Rad, L.; Irani, M.; Haririan, I. *J. Appl. Polym. Sci.* **2015**, *132*, DOI: 10.1002/app.41286.
8. TaytonPurcell, E. E.; Aarvold, A. M.; Smith, J. O.; Briscoe, A.; Kanczler, J. M.; Shakesheff, K. M.; Howdle, S. M.; Dunlop, D. G.; Oreffo, 1, R. O. C. *J. Biomed. Mater. Res. A* **2014**, *102*, 2613.
9. Mouriño, V.; Cattalini, J. P.; Roether, J. A.; Dubey, P.; Roy, I.; Boccaccini, A. R. *Expert Opin. Drug Deliv.* **2013**, *10*, 1353.
10. Liuyun, J.; Chengdong, X.; Lixin, J.; Lijuan, X. *Compos. Sci. Technol.* **2014**, *93*, 61.
11. Balaji Raghavendran, H. R.; Puvaneswary, B.; Talebian, S.; Raman Murali, M.; Vasudevaraj Naveen, S.; Krishnamurithy, G.; McKean, R.; Kamarul, T. *PLoS One* **2014**, *9*, e104389.
12. Qi, H.; Ye, Z.; Ren, H.; Chen, N.; Zeng, Q.; Wu, X.; Lu, T. *Life Sci.* **2016**, *148*, 139.
13. Motealleh, B.; Zahedi, P.; Rezaeian, I.; Moghimi, M.; Abdolghaffari, A. M.; Zarandi, M. A. *J. Biomed. Mater. Res. B* **2014**, *102*, 977.
14. Jin, G.; Prabhakaranb, M. P.; Kai, D.; Annamalai, S. K.; Arunachalam, K. D.; Ramakrishna, S. *Biomaterials* **2013**, *34*, 724.
15. Nguyen, T. T. T.; Ghosh, C.; Hwang, S.-G.; Dai Tran, L.; Park, J. S. *J. Mater. Sci.* **2013**, *48*, 7125.
16. Han, Q.-Q.; Du, Y.; Yang, P.-S. *Future Med. Chem.* **2013**, *5*, 1671.
17. Suganya, S.; Venugopal, J.; Ramakrishna, S.; Lakshmi, B. S.; Giri Dev, V. R. *J. Appl. Polym. Sci.* **2014**, *131*, DOI: 10.1002/app.39835.
18. Wirries, A.; Schubert, A.-K.; Zimmermann, R.; Jabari, S.; Ruchholtz, S.; El-Najjar, N. *Int. Immunopharmacol.* **2013**, *15*, 381.
19. Bessa Pereira, C.; Gomes, P. S.; Costa-Rodrigues, J.; Almeida Palmas, R.; Vieira, L.; Ferraz, M. P.; Lopes, M. A.; Fernandes, M. H. *Cell Prolif.* **2012**, *45*, 386.
20. Costa-Rodrigues, J.; Carmo, S. C.; Silva, J. C.; Fernandes, M. H. R. *Cell Prolif.* **2012**, *45*, 566.
21. Wang, X.-L.; Wang, N.-L.; Zhang, Y.; Gao, H.; Pang, W.-Y.; Wong, M.-S.; Zhang, G.; Qin, L.; Yao, X.-S. *Chem. Pharm. Bull.* **2008**, *56*, 46.
22. Zhang, D.-W.; Cheng, Y.; Wang, N.-L.; Zhang, J.-C.; Yang, M.-S.; Yao, X.-S. *Phytomedicine* **2008**, *15*, 55.
23. Udalamaththa, V.; Jayasinghe, C.; Udagama, P. *Stem Cell Res Ther.* **2016**, *7*, 1.
24. Badole, S.; Kotwal, S. *Int. J. Pharm. Sci. Health Care* **2014**, *1*, 131.
25. Asgarpanah, J.; Roohi, E. *J. Med. Plants Res.* **2012**, *6*, 3942.
26. Asgharikhatooni, A.; Bani, S.; Hasanpoor, S.; Mohammad Alizade, S.; Javadzadeh, Y. *Iran Red Crescent Me.* **2015**, *17*, e25637.
27. Quettier-Deleu, C.; Gressier, B.; Vasseur, J.; Dine, T.; Brunet, C.; Luyckx, M.; Cazin, M.; Cazin, J.-C.; Bailleul, F.; Trotin, F. *J. Ethnopharmacol.* **2000**, *72*, 35.
28. Mohanty, A. K.; Misra, M.; Drzal, L. T. Natural Fibers, Biopolymers, and Biocomposites; CRC Press, New York, **2005**.
29. Park, J.-Y.; Lee, I.-H. *J. Polym. Res.* **2011**, *18*, 1287.
30. Reise, M.; Wyrwab, R.; Müller, U.; Zylinski, M.; Völpel, A.; Schnabelrauch, M.; Berg, A.; Jandt, K. D.; Watts, D. C.; Sigusch, B. W. *Dent. Mater.* **2011**, *28*, 179.
31. Jeong, Y.; Chan, Y.; Taek, K.; Sup, J. *Biochem. Pharma.* **2006**, *72*, 1268.
32. Zhang, Z.-Y.; Teoh, S.-H.; Chong, M. S. K.; Schantz, J. T.; Fisk, N. M.; Choolani, M. A.; Chan, J. *Stem Cells* **2009**, *27*, 126.